

Lung pathology of natural *Babesia rossi* infection in dogs

C Martin,¹ S Clift,² A Leisewitz^{3,4}

¹ Idexx Laboratories (Pty) Ltd, South Africa

² Section of Pathology, Department of Paraclinical Sciences, Faculty of Veterinary Science, University of Pretoria, South Africa

³ Department of Clinical Sciences, Bailey Small Animal Teaching Hospital, Auburn University College of Veterinary Medicine, United States of America

⁴ Section of Small Animal Medicine, Companion Animal Clinical Sciences, Faculty of Veterinary Science, University of Pretoria, South Africa

Corresponding author, email: all0087@auburn.edu

A proportion of *Babesia rossi* infections in dogs are classified as complicated and one of the most lethal complications is acute lung injury (ALI) and acute respiratory distress syndrome (ARDS). Most dogs that die succumb within 24 hours of presentation. The pulmonary pathology caused by *B. rossi* in dogs has not been described. The aim of this study was to provide a thorough macroscopic, histological and immunohistochemical description of the lung changes seen in dogs naturally infected with *B. rossi* that succumbed to the infection. Death was invariably accompanied by alveolar oedema. Histopathology showed acute interstitial pneumonia characterised by alveolar oedema and haemorrhages, with increased numbers of mononuclear leucocytes in alveolar walls and lumens. Intra-alveolar polymerised fibrin aggregates were observed in just over half the infected cases. Immunohistochemistry showed increased numbers of MAC387- and CD204-reactive monocyte-macrophages in alveolar walls and lumens, and increased CD3-reactive T-lymphocytes in alveolar walls, compared with controls. These histological features overlap to some extent (but far from perfectly) with the histological pattern of lung injury referred to as the exudative stage of diffuse alveolar damage (DAD) as is quite commonly reported in ALI/ARDS.

Keywords: ALI, ARDS, babesiosis, immunohistochemistry, interstitial pneumonia, pulmonary

Introduction

The typical clinicopathological hallmarks of uncomplicated canine babesiosis include lethargy, mild to moderate haemolytic anaemia with a water-hammer pulse, pyrexia and splenomegaly without signs of organ failure/dysfunction (Leisewitz et al. 2019b). The complicated form includes evidence of organ failure/dysfunction such as severe anaemia, acute renal failure, haemorrhagic encephalomalacia, icterus, haemoconcentration, disseminated intravascular coagulation, acute pancreatitis, myocardial infarction as well as pulmonary oedema (Leisewitz et al. 2019; Welzl et al. 2001). These complicated forms appear to be triggered by the host inflammatory response and cannot be directly attributed to anaemia alone (Jacobson & Clark 1994; Leisewitz et al. 2019a). Maegraith et al. (1957) first described the pulmonary pathology in dogs that died from what we now refer to as complicated canine babesiosis as early as 1957 in dogs experimentally infected with what was most likely *B. rossi*. In that paper, 25/34 dogs showed some pulmonary pathology varying from slight hyperaemia to severe pulmonary oedema, especially in the fatal cases. So called “shock lung” or acute interstitial pneumonia has long been recognised as a significant lesion in complicated canine babesiosis infection but the pathology has never been investigated or described.

Acute lung injury (ALI) and acute respiratory distress syndrome (ARDS) are clinical syndromes characterised by arterial hypoxaemia caused by pulmonary pathology that leads to a reduction in the efficiency of gaseous exchange (Wilkins et al. 2007). Diagnosis of ALI and ARDS can only be reached if cardiac causes of dyspnoea have been ruled out (Wilkins et al. 2007). It is important to realise that ALI and ARDS are on a continuum,

with ALI being less severe than ARDS, but as the pulmonary injury and hypoxaemia worsens, ALI progresses to ARDS. ALI and ARDS are infrequently observed in veterinary medicine, but they are commonly fatal. It is not a diagnosis in and of itself but is rather the endpoint of a variety of diseases and conditions that are responsible for the underlying lung pathology. Recognising when the syndrome is present is important from a treatment and prognosis point of view. ALI and ARDS should be a differential diagnosis for any dog presenting with acute onset severe dyspnoea.

ALI and ARDS were first described by Ashbaugh et al. (1967) in 1967 in human patients. An adult respiratory distress syndrome was initially described but eventually the clinical term Acute Respiratory Distress Syndrome was coined because it was also found to occur in children (Ware & Matthay 2000). Since these initial studies, a vast amount of research has been done as ALI/ARDS is still a leading cause of mortality in human medicine. It is estimated that 40–60% of human patients diagnosed with these syndromes, despite all the latest technological advances, will die as a result (Ware & Matthay 2000). There are numerous potential risk factors which may predispose to ALI/ARDS. One of the most common and well-characterised is systemic bacterial infection or sepsis and septic shock (Castro 2006; Thille et al. 2013; Ware 2006) which occur in all species, especially in immunocompromised patients. The lipopolysaccharides or endotoxins of Gram-negative infections in systemic circulation are a well described trigger. ALI and ARDS are important causes of death in human *Plasmodium* spp. infection (mostly *P. falciparum* and less commonly *P. vivax* (Anstey et al. 2007)) and have been extensively studied (Van den Steen et al. 2013). Malaria and babesiosis have similarities in that they are both caused by vector-borne haemoprotzoal parasites

belonging to the phylum Apicomplexa. Many manifestations of disease have a shared pathogenesis and evoke a similar host immune response (Krause et al. 2007). Murine models exist for both *Plasmodium* and *Babesia* infection and the lesions observed show striking similarities.

In the human and veterinary literature, the type of lesion most commonly associated with ALI/ARDS is diffuse alveolar damage (Castro 2006; Ware & Matthay 2000). However, other pulmonary pathology such as diffuse interstitial pneumonia and non-cardiogenic pulmonary oedema can also result in arterial hypoxaemia. Diffuse alveolar damage can be grouped according to three temporal stages depending on the time that has elapsed since the initial insult and the subsequent chronological development of lesions (Castro 2006; Thille et al. 2013; Tomaszewski Jr 2000; Ware & Matthay 2000). More than one phase can be present at any one time. The three stages include an acute exudative stage, followed by a sub-acute proliferative stage and finally a chronic fibrotic stage. Most research has been devoted to the acute stage lung injury in dogs as the proliferative and fibrotic phases of ALI/ARDS are not often encountered in veterinary medicine. In human medicine, due to more advanced interventions and treatments that lead to increased survival times, the later stages of the disease are encountered more commonly.

The pathology and pathophysiology of ALI/ARDS due to *Babesia* and malaria infection have been studied in humans (Taylor et al. 2012; Van den Steen et al. 2013) as well as in murine models (Aitken et al. 2014; Hemmer et al. 1999; Lovegrove et al. 2008; Souza et al. 2013; Van den Steen et al. 2010). Here we provide the first detailed description of the gross pathology, histopathology and selected immunohistochemical (IHC) features of naturally fatal *B. rossi* infection in dogs and show that it is indeed characteristic of diffuse alveolar damage (DAD) typical of ALI (in the less severely affected dogs) and ARDS (in the more severely affected dogs). Previous descriptions are dated (and hence no molecular confirmation of a mono-infection with *B. rossi* was possible) or, if *B. rossi* was confirmed, descriptions were of the gross pathology only.

Materials and methods

Case selection

This project was a prospective cohort descriptive case control study on 11 dogs naturally infected with *B. rossi* that died or were euthanised due to complicated disease. Complicated disease has previously been defined by Leisewitz et al. (2019b). Briefly, it includes dogs that are sick enough to require hospital admission that show clinical and biochemical evidence of significant organ dysfunction or failure. Infected dogs (infected group – IG) were sourced from the Onderstepoort Veterinary Academic Hospital (OVAH). They included nine different breeds, seven intact females and four intact males with a median age of three years (range 0.3–9 years). All were diagnosed with the infection based on a positive stained (Diff-Quick) thin blood smear and only dogs with a *B. rossi* mono-infection (based on a PCR and reverse line blot assay capable of detecting a range of *Babesia*, *Theileria*, *Anaplasma* and *Ehrlichia* spp.) were selected for investigation (Matjila et al. 2008).

Other exclusion criteria included: Any animal that received treatment for *Babesia* in the four weeks preceding presentation to the OVAH; any animal that received steroidal or non-steroidal treatment in the four weeks preceding their presentation and, finally, any animal that was suspected or confirmed to have a comorbid infectious disease. The control group (CG) included four dogs that were euthanised at a shelter welfare organisation or the OVAH on humane grounds. Dogs were all medium sized, mixed breeds, of unknown age (but estimated to be between one and three years of age). Dogs were automatically excluded from the control group if any blood parasite was diagnosed by PCR or if any significant comorbid disease was diagnosed clinically or at post mortem. This study was approved by the animal ethics committee of the University of Pretoria (V073-16).

Sample collection

A standard post-mortem examination was performed within an interim of 18 hours. The lungs were first photographed and then histopathology specimens were collected as quickly as possible to minimise alveolar collapse and autolysis. Samples were collected using a sharp knife to minimise tissue crush artefact. Two 1 cm³ samples, taken from the most severely affected areas of each lobe of the left and right lung, were fixed in 10% neutral buffered formalin for 2–6 days. Lung tissue was not fixed artificially inflated but in its natural state, collected directly from the cadaver specimen. Immediately after sampling for histopathology, the lungs were carefully palpated and the macroscopic pathology described in detail.

Histopathology

Tissue processing, embedding, sectioning and staining for histopathology was performed according to standard laboratory procedures (Bancroft & Gamble 2008). For routine light microscopy, 4 µm-thick tissue sections were stained with hematoxylin and eosin (H&E). Preliminary histological evaluation of all the samples showed that lesions were relatively uniformly distributed throughout all the lung lobes (data not shown). However, we measured alveolar wall thickness in all four lung lobes and the left caudal lobe had the least variation (data not shown), so sections from this lobe were selected for further detailed histological analysis and IHC staining.

Immunohistochemistry

A manual chromogen-based indirect immunoperoxidase staining technique was performed as previously described (Henning et al. 2020), according to international recommended guidelines for veterinary IHC laboratories (Ramos-Vara et al. 2008; Ramos-Vara & Miller 2014). Antibody species specificity has been documented in previous studies and recorded by manufacturers (Henning et al. 2020; Jubala et al. 2005; Ramos-Vara et al. 2007). Briefly, lung tissues from the infected and control dogs were deparaffinised, treated with 3% hydrogen peroxide in methanol for 15 minutes, and then heated with citric acid (pH 6.0) or ethylenediaminetetraacetic acid (EDTA; pH 9.0), using a microwave oven for antigen retrieval. Selected antibodies (CD3, CD20, CD204, MUM1, myeloid/histiocyte antigen [MAC387], Pax-5 and VCAM-1) were applied to the lung specimens (antibody details, dilutions and incubation times as

previously reported (Henning et al. 2020); followed by rinsing in distilled water, then in 0.1 M PBS (pH 7.6), containing 0.1% bovine serum albumin (BSA) buffer solution. Slides were further treated according to the BioGenex (Catalogue no. QD420-YIKE, Fremont, CA, USA) or EnVision (Catalogue no. K5007, Dako, Glostrup, Denmark) polymer kit instructions, and bound peroxidase was detected with 3,3'-diaminobenzidine tetrahydrochloride (DAB) (Catalogue no. K3468, Dako, Glostrup, Denmark). Sections were counterstained with Mayer's haematoxylin for 20 seconds. Positive dog tissue control specimens included reactive lymph node (for the lymphocyte and monocyte-macrophage markers) and granulation tissue (for VCAM-1), and, for negative reagent control purposes, sections were stained without primary antibody.

Data analysis

Pertaining to the IHC-stained slides, the number of immunoreactive cells for each of the major regions of interest (alveoli, alveolar walls and peribronchial interstitium) were counted in five 400 × fields and averaged. The same procedure was used on the control lungs to establish an average as well as a standard deviation, which was subsequently used to create a normal range for non-diseased lungs (hence the normal range was regarded as the mean plus one standard deviation). Where IHC was not scored (VCAM-1), the pattern of immunoreactivity was described and compared with control lungs.

Results

Gross pathology

Lesions varied greatly among cases, but multifocal, often coalescing haemorrhages were a consistent finding resulting in a dark red, mottled appearance to the lungs (Figure 1A). Severe diffuse haemorrhage was also noted in some cases (Figure 1B). Severe pulmonary oedema, as evidenced by increased weight and consistency of lung tissue, as well as oozing of blood-stained frothy fluid on cut section (Figure 1C), and accumulation of tracheal froth (Figure 1D), was also a consistent finding.

Histopathology

Overview

Most cases exhibited moderate to severe protein-rich pulmonary oedema (Figure 2A) and multifocal to coalescing, and occasionally focally extensive haemorrhage/s (Figure 2B). The proteinaceous nature of the exudate was assessed histologically and not measured in an objective quantitative way. In the majority of cases, alveolar macrophages were markedly increased (Figure 2C); they were often vacuolated and haemosiderin-laden. Intra-alveolar neutrophils were seen in only two of 11 cases.

The alveolar interstitium was consistently markedly thickened due to increased mononuclear leukocytes in both the extra- and intravascular compartments (Figures 2D and E). Intravascular megakaryocytes and haemosiderin-containing monocytes were commonly observed. Lung specimens were often moderately to severely congested, with moderate to severe widespread vascular endothelial cell activation (hypertrophy),

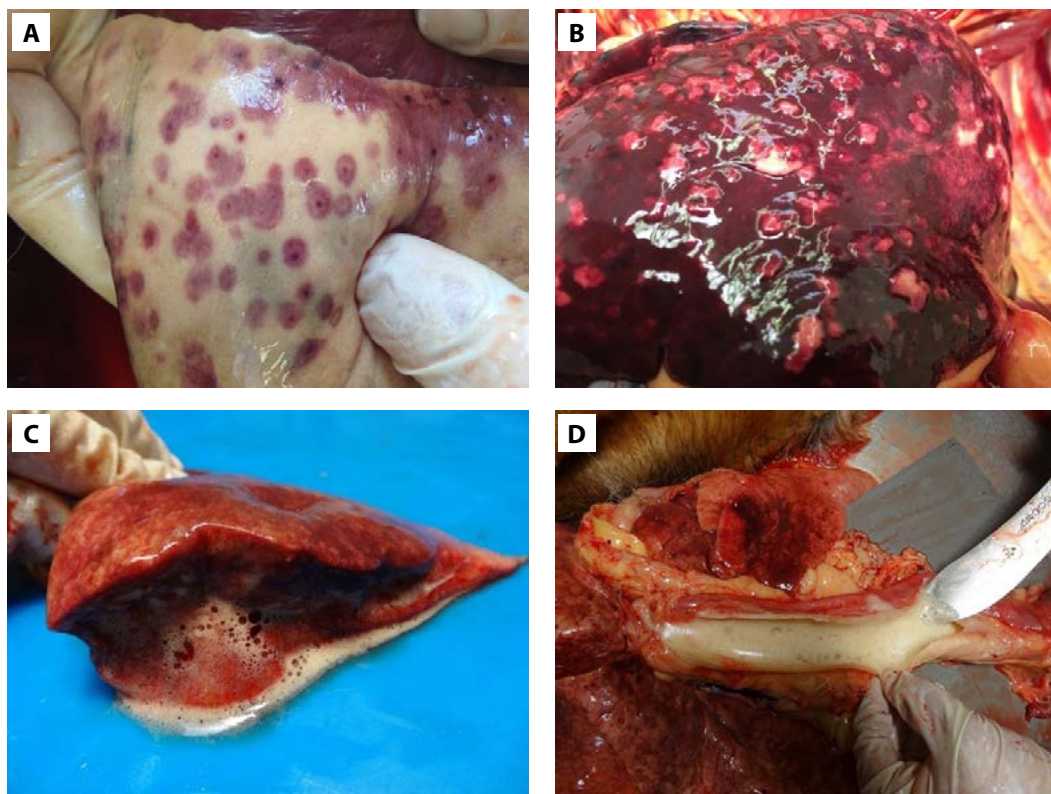


Figure 1 A–D: Macroscopic pathology of the lungs of *Babesia rossi*-infected dogs; (A) Multifocal to coalescing haemorrhages and diffuse lung pallor (suggestive of anaemia); (B) Severe diffuse haemorrhage; (C) Severe oedema with frothy fluid oozing from the cut surface; (D) Froth-filled trachea, indicative of severe terminal lung oedema

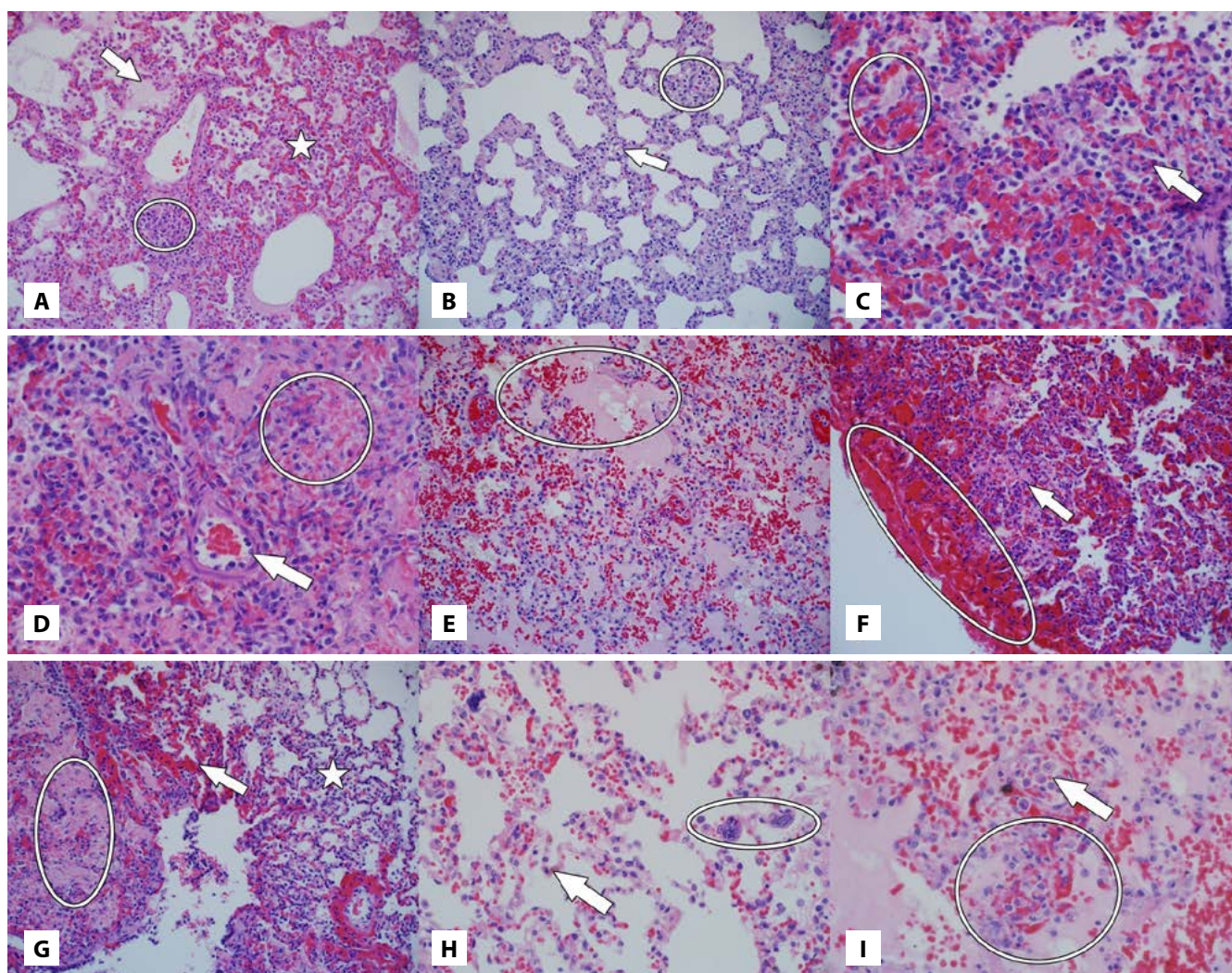


Figure 2 A–I: Photomicrographs of H&E stained tissue sections of the lungs of dogs that died of *Babesia rossi* infection; (A) Focal severe alveolar macrophage infiltration (star) with pulmonary oedema (arrow) and mild interstitial expansion due to perivascular lymphocyte and plasma cell accumulation (circle), 200 × magnification HE; (B) Moderate thickening of the alveolar walls due to mononuclear leukocytic infiltration (arrow) with endothelial cell activation and leukostasis (circle), 200 × magnification HE; (C) Severe mononuclear alveolar inflammatory cell infiltrate characterised by alveolar macrophages and fewer neutrophils (arrow) with haemorrhage and fibrin exudation extending into the alveolar ducts (circle), 400 × magnification HE; (D) Severe mononuclear alveolar inflammatory cell infiltrate with haemorrhage and fibrin exudation (circle) as well as endothelial cell activation, lymphocyte margination (arrow) and perivascular infiltration, 400 × magnification HE; (E) Severe accumulation of moderately protein-rich alveolar oedema with moderate haemorrhage (circle), 200 × magnification HE; (F) Subpleural haemorrhage (circle), severe alveolar infiltrate with haemorrhage (arrow), 200 × magnification HE; (G) Mild bronchiolar haemorrhage (arrow) with alveolar fibrin exudation (circle) and moderate alveolar mononuclear cell infiltrate (star), 200 × magnification HE; (H) Intravascular haemosiderophages (arrow) and megakaryocytes (circle), 400 × magnification HE; (I) Severe interstitial mononuclear expansion with endothelial cell activation and intravascular mononuclear leukostasis (arrow), moderate alveolar haemorrhage and fibrin and severe accumulation of high protein content pulmonary oedema (circle), 400 × magnification HE

and multifocal intra-alveolar fibrin exudation (Figures 2F and G). Mild perivascular oedema was also frequently visible. *Babesia rossi* intraerythrocytic piroplasms were visible in only three of 11 cases, and cell death in alveolar septa, characterised by karyorrhexis and karyolysis, was rarely observed.

Bronchioles often contained oedema, fibrin and haemorrhage, and, occasionally, a few neutrophils. Mild to moderate perivascular lymphoplasmacytic cuffing was evident in only two of 11 cases. Dark brown to black, refractive intracytoplasmic carbon pigment was present in macrophages in the bronchus-associated lymphoid tissue, consistent with anthracosis. In one case, a large fibrin thrombus was observed in the peri-bronchial

vasculature. Atelectasis and a few foci of alveolar emphysema were seen in a small number of cases.

Lesion scoring

Autolysis was mild in all control and infected samples. Congestion was mild in 6/11 cases (54.5%), moderate in 2/11 cases (18.2%), and absent in the remaining 3/11 cases (27.3%).

Within the alveolar walls, the inflammatory cell infiltrate, apoptosis and microvascular endothelial activation was scored along with the presence or absence of thrombosis. Monocyte-macrophage infiltration was severe in 2/11 (18.2%) of cases, moderate in 2/11 (18.2%), mild in 6/11 (54.5%) and absent in 1/11 (9.1%). Lymphocyte infiltration was moderate in 1/11 (9.1%), mild in 5/11 (45.5%) and absent in 5/11 (45.5%), while plasma cell

infiltrates were mild in 2/11 (18.2%) and absent in 9/11 (81.8%) of cases. Neutrophils and eosinophils were extremely scarce in all 11 cases. Cell death was moderate in 1/11 (9.1%), mild in 8/11 (72.7%) and not visible in 2/11 (18.2%) of cases. Nuclear hypertrophy/activation was severe in 2/11 (18.2%), moderate in 6/11 (54.5%) and mild in 3/11 (27.3%). Thrombosis was present in 2/11 (18.2%) and absent in 9/11 (81.8%) of cases.

Similar inflammatory cell parameters were evaluated in the alveolar lumens, as well as fibrin exudation, haemorrhage, oedema and hyaline membrane formation. Monocyte-macrophage infiltrates were severe in 1/11 (9.1%), moderate in 5/11 (45.5%) and mild in 5/11 (45.5%) of cases. Neutrophilic inflammation was mild in 2/11 (18.2%) and absent in 9/11 (81.8%) of cases. Lymphocytes, plasma cells and eosinophils were absent in all cases. Fibrin exudation was severe in 1/11 (9.1%), moderate in 3/11 (27.3%), mild in 2/11 (18.2%) and absent in 5/11 (45.5%) cases. Alveolar haemorrhage was severe in 2/11 (18.2%), moderate in 2/11 (18.2%), mild in 5/11 (45.5%) and absent in 2/11 (18.2%) cases. Additionally, haemorrhage was multifocal in 7/9 (77.8%), coalescing in 1/9 (11.1%) and diffuse in 1/9 (11.1%) cases. Oedema was severe in 8/11 (72.7%), moderate in 1/11 (9.1%) and mild in 2/11 (18.2%) cases. True hyaline membranes were not seen in any of the cases.

The perivascular interstitium was also evaluated for inflammatory cells, fibrin, haemorrhage, oedema, microvascular endothelial cell activation and lymphatic distension. Monocyte-macrophage infiltrates were moderate in 2/11 (18.2%), mild in 3/11 (27.3%) and absent in 6/11 (54.5%) cases. Lymphocytic inflammation was moderate in 2/11 (18.2%), mild in 3/11 (27.3%) and absent in 6/11 (54.5%) cases. Plasma cell inflammation was mild in 4/11 (36.4%) and absent in 7/11 (63.6%) cases. Neutrophils and eosinophils were absent in all cases. Fibrin exudation was mild in 2/11 (18.2%) and absent in 9/11 (81.8%) cases. Haemorrhage was mild in 2/11 (18.2%) and absent in 9/11 (81.8%). Distribution of haemorrhage was multifocal in both cases. Oedema was severe in 1/11 (9.1%), moderate in 3/11 (27.3%), mild in 6/11 (54.5%) and absent in 1/11 (9.1%) cases. Endothelial cell nuclear activation was severe in 1/11 (9.1%), moderate in 6/11 (54.5%) and mild in

4/11 (36.4%) cases. Lymphatic vessel dilation was absent in all but 1/11 (9.1%) cases, in which it was mild.

The subpleural interstitium was evaluated for inflammatory cells, fibrin, haemorrhage, oedema and mesothelial activation. No monocytes-macrophages, lymphocytes, plasma cells, neutrophils or eosinophils were present. Fibrin exudation was moderate in 1/11 (9.1%) and absent in 10/11 (90.9%) cases. Haemorrhage was absent in 10/11 (90.9%) and moderate in 1/11 (9.1%) cases, in which it was multifocal. Oedema was mild in 5/11 (45.5%) and absent in 6/11 (54.5%) cases. Pleural mesothelial activation was only seen in 1/11 (9.1%) cases.

The peribronchiolar interstitium was also evaluated for inflammatory cells, fibrin, haemorrhage, oedema and anthracosis. Monocyte-macrophages, lymphocytes, plasma cells, neutrophils and eosinophils were absent in all cases. Fibrin exudation was mild in 1/11 (9.1%) and absent in 10/11 (90.9%) cases. Haemorrhage was absent in 10/11 (90.9%) and mild in (1/11) 9.1% cases and the distribution was multifocal. Oedema was absent in all cases. Anthracosis was present in 5/11 (45.5%) and absent in 6/11 (54.5%) cases.

Bronchiolar lumens were evaluated for inflammatory cells, fibrin, haemorrhage and oedema. Monocyte-macrophage inflammation was mild in 1/11 (9.1%) and absent in 10/11 (90.9%) cases. No lymphocytes, plasma cells, neutrophils or eosinophils were present. No fibrin exudate was visible either. Haemorrhage was absent in 4/11 (36.4%) and mild in 7/11 (63.6%) cases and the distribution was focal in 4/7 (57.1%) and multifocal in 3/7 (42.9%) cases.

Immunohistochemistry

The most significant results are summarised in Table I.

MAC387

Within the alveolar lumens, the MAC387-reactive bone marrow-derived monocyte-macrophages (and scarce neutrophils) ranged from 1.2 to 58.6/HPF (400x magnification) with an average of 11.8 cells/HPF, which is an increase of 10.8 × compared to the controls

Table I: Summary of significant results of the immunohistochemical pathology of the lungs of dogs naturally infected with *Babesia rossi* that died as a result of the infection, all cell counts were averaged over five high power fields per histological compartment (approximately 1.185 mm² per compartment)

Antibody	Compartment	<i>Babesia</i> -infected dogs (mean and range)	Control dogs (mean and range)	Increase magnitude in <i>Babesia</i> -infected dogs
MAC387	Alveolar lumen	11.8 (9.8–33.4)	0.6 (0–1.2)	10.8 × increase
	Alveolar wall	59.6 (25.4–93.7)	8.9(3–14.8)	44.6 × increase
	Peribronchial interstitium	1.9 (0.1–3.6)	3.45 (0–7)	Normal
CD204	Alveolar lumen	7.4 (3–12)	0.95 (0–1.9)	3.9 × increase
	Alveolar wall	5.3 (1–10)	0.1 (0–0.4)	5.3 × increase
	Peribronchial interstitium	Peribronchial interstitium	0.4 (0–1.1)	Normal
CD3	Alveolar lumen	0.0 (0–0)	0 (0–0)	Normal
	Alveolar wall	12.4 (0–24.8)	0 (0–0)	12.4 × increase
	Peribronchial interstitium	0.1	0.2 (0.0)	Normal
CD20	Alveolar lumen	2.2 (0.2–4.7)	0.9 (0–2)	2.2 × increase
	Alveolar wall	2.5 (0.9–6)	(0 (0–0)	2.5 × increase
	Peribronchial interstitium	0.5	1.2 (0–3)	Normal

(Figure 3A & B). Positive cells in the alveolar walls ranged from 0.8 to 140.4/HPF with an average of 59.6 cells/HPF, which is a 4 × increase compared to the normal controls. MAC387-reactive leukocytes in the peribronchial regions ranged between 0.4 and 4.4 cells/HPF with an average of 1.9 cells/HPF which falls within the normal range established in the control sections.

CD204

The number of CD204-positive macrophages in alveolar septa ranged from 0.2 to 12/HPF with an average of 5.3 cells/HPF, which is a 5.3 × increase compared to the normal controls (Figure

3C & D). Positive cells in alveolar lumens ranged from 0 to 12.2/HPF with an average of 7.4 cells/HPF, which is a 3.9 × increase compared to the normal controls.

CD3

In the alveolar septa of *B. rossi*-infected dogs, 1.4–29.4 CD3 positive T-lymphocytes were counted/HPF with an average of 12.4 T-lymphocytes/HPF (Figure 3E–F). This is a 12.4 × increase compared to the normal range established in the uninfected controls. Between 0 and 0.4 T-lymphocytes were counted/HPF in the peribronchial regions, which was within the normal range

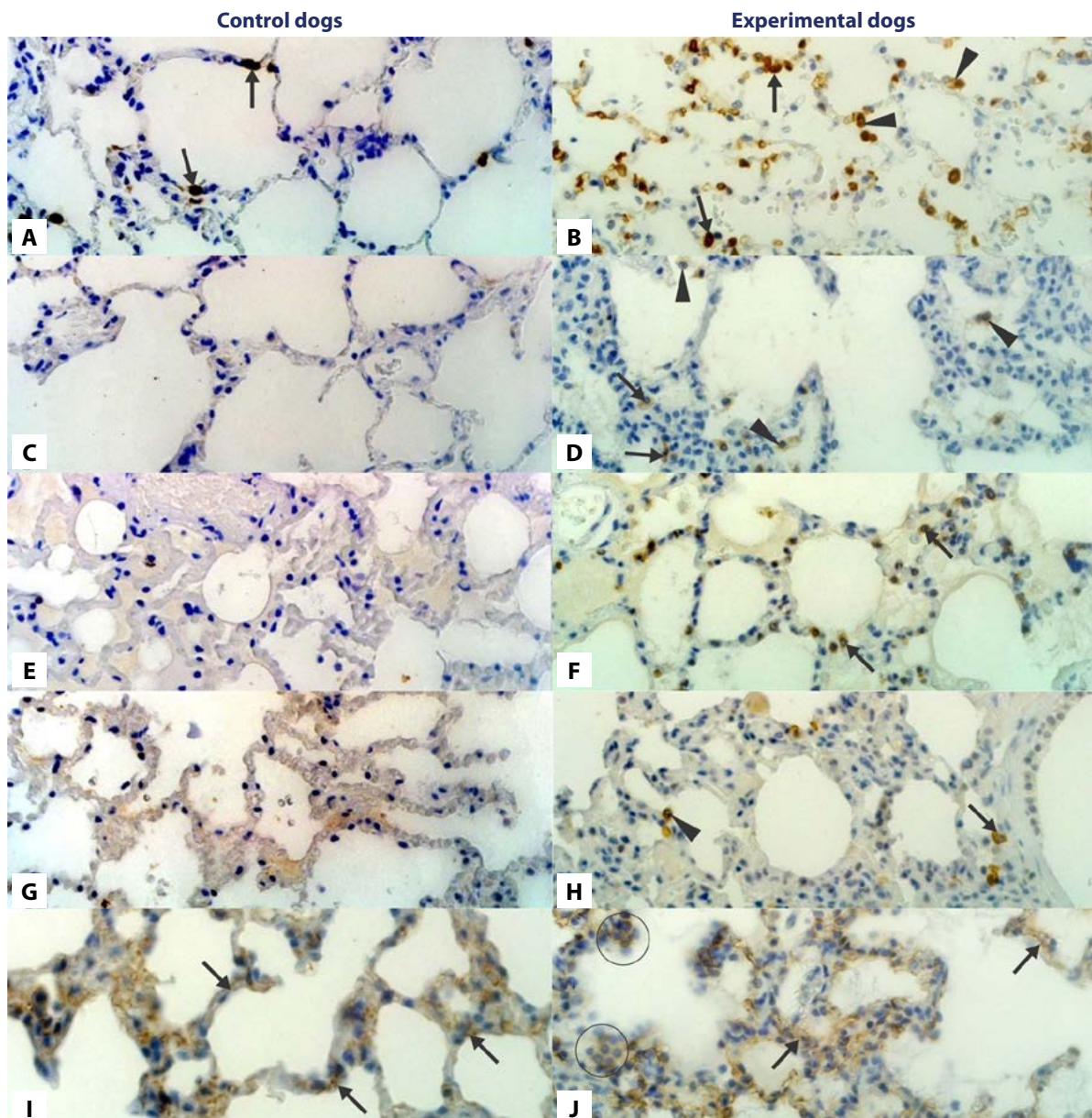


Figure 3: Immunohistochemical labelling of leukocytes and vascular endothelial cells in the lungs of representative *Babesia rossi*-infected dogs (right) compared to uninfected controls (left). 3,3'-diaminobenzidine tetrahydrochloride (DAB) chromogen, 400 × magnification; (A) MAC387-reactive mononuclear leukocytes in the alveolar septa of the control dog lung (arrows); (B) Increased MAC387-reactive mononuclear leukocytes (and rare neutrophils) in the alveolar septa (arrows) and alveolar lumens (arrowheads) of an infected dog; (C) No CD204 reactivity in alveolar septa or lumens in uninfected control tissue; (D) CD204-reactive alveolar mononuclear leukocytes in the alveolar septa (arrows) and alveolar lumens (alveolar macrophages; arrowheads) of an infected dog; (E) No CD3-reactive T-lymphocytes were observed in alveolar lumens or alveolar walls in uninfected controls; (F) CD3-reactive T-lymphocytes in the alveolar septa of an infected dog (arrows); (G) No CD20-reactive B-lymphocytes in alveolar lumens or alveolar septa in the control lung sample; (H) CD20-reactive B-lymphocytes/plasma cells in the alveolar septa (arrow) and alveolar lumen (arrowhead) in an infected dog; (I) VCAM-reactive microvascular endothelial cells in uninfected control lung tissue (arrows); (J) VCAM-1-reactive endothelial cells (arrows) and intravascular mononuclear leukocytes (circles) in alveolar septa

established in the controls. Within the alveolar lumens, there were no CD3-positive T-lymphocytes in any of the naturally infected cases, which is no different from the normal control cases.

CD20

The alveolar walls contained from 0 to 7.6 CD20-positive B-lymphocytes and/or plasma cells/HPF with an average of 2.5 cells/HPF which is 2.5 × increase compared to the controls (Figure 3G & H). There were 0 to 7.4 CD20-reactive cells/HPF with an average of 2.2 cells/HPF in the alveolar lumens, which is a 2.2 × increase compared to the controls. In the peribronchial regions, there were 0–1 positive B-lymphocytes and plasma cells with an average of 0.5 cells/HPF, which falls within the range observed in the uninfected control group.

MUM-1

MUM1-positive mature B-lymphocytes and/or plasma cells ranged from 0–5.4/HPF in the alveolar walls, with an average of 1.6 cells/HPF, which is a 0.6 × increase compared to the controls. Positive cells in the peribronchial regions varied from 0–2.8/HPF with an average of 0.6 cells/HPF, which is a 0.6 × increase over the control cases. There were no MUM1-positive cells in the alveolar lumens, which is no different from the normal controls.

VCAM-1

In most *B. rossi*-infected lung specimens, microvascular endothelial cells were intensely VCAM-1-reactive, with positive labelling occurring in almost parallel lines in alveolar septa. However, the staining pattern was essentially similar to that in the control lung specimens (Figure 3I & J). Unlike the control cases however, the naturally infected cases did exhibit granular, usually membranous positivity in intravascular mononuclear leukocytes (Figure 3J).

In summary, the lungs of naturally infected *B. rossi* dogs exhibited increased numbers of MAC387-positive monocyte-macrophages (and rare neutrophils), CD204-positive macrophages and CD3-positive T-lymphocytes when compared to the lung specimens from normal uninfected control dogs. Milder increases in CD20-positive B-lymphocytes and/or plasma cells were also noted.

Discussion

At the macroscopic level, there was some variability in the appearance of the lungs in dogs with babesiosis, but most infected cases in this series showed moderate to severe multifocal pulmonary haemorrhages. Severe pulmonary oedema, as evidenced by oozing of fluid on cut section as well as copious, often blood-tinged, tracheal froth was present as well. Consequently, the lungs were often heavy with a slightly increased consistency. Acute interstitial pneumonia with oedema, congestion and multifocal haemorrhage was reported in 16 of 25 (64%) post-mortems conducted in the largest case series of *B. rossi* infected dogs (Leisewitz et al. 2019b). That study, which only evaluated gross post-mortem changes, also described pleural and pericardial effusions in 9/25 (36%) and 4/25 (16%) of cases at post mortem (Leisewitz et al. 2019b). In an older study that demonstrated the multisystemic nature of the

disease in 91 complicated cases, 32 died (35%), 18 of them (20%) due to respiratory failure (Welzl et al. 2001). Although it was not evaluated in the current study, arterial blood gas analysis evaluating acid-base and lung function has been studied in *B. rossi* infection previously, and the classic findings of ARDS were not commonly diagnosed (Leisewitz et al. 2001). This was probably due to the fact that the time of arterial blood collection in these cases was many hours before death, whilst ARDS (associated with widespread alveolar flooding and tracheal foam) appears to be a terminal event in this disease. ALI seems very common, as many cases dying of organ failure in complicated canine babesiosis, other than lung failure, demonstrate pulmonary pathology consistent with ALI (Leisewitz et al. 2001). The most common blood gas disturbance seen in severe disease is respiratory alkalosis mixed with metabolic acidosis which is consistent with primary metabolic and pulmonary pathology (Leisewitz et al. 2001).

The described changes were similar to the macroscopic pathology noted in human malaria-associated ARDS where severe oedema and intrapulmonary haemorrhages are described (Taylor et al. 2012). ARDS has been described in 8% of 139 cases of human *B. microti* infection (White et al. 1998). Murine malaria-associated ARDS in C57BL/6J mice infected with *Plasmodium berghei* NK65 showed petechial haemorrhages (Van den Steen et al. 2010). The pathology noted in a murine model of *Babesia*-associated ALI/ARDS in C3H/HeN mice infected with WA-1 *Babesia* showed petechiations with serosanguinous fluid in the trachea and bronchi (Hemmer et al. 1999), which is similar to the haemorrhage and pulmonary oedema noted in canine babesiosis.

In general, histological sections of lung all showed multifocal haemorrhages and severe pulmonary oedema correlating with the macroscopic findings. Alveolar septa were commonly thickened due to infiltration of mononuclear inflammatory cells, dominated by MAC387- and CD204-positive monocyte-macrophages (which were 4x and 5.3x increased respectively, compared to normal controls). These findings are strikingly different to a typical bacterial pneumonia which is dominated by a neutrophilic infiltrate.

Pulmonary oedema was the most consistent feature of *Babesia*-associated lung injury. This correlates with human malaria-associated ARDS (Taylor et al. 2012), a murine model of MA-ARDS in C57BL/6j mice infected with *Plasmodium berghei* (Van den Steen et al. 2010), and a murine model of babesiosis in which C3H/HeN mice were infected with WA-1 *Babesia* (Hemmer et al. 2000; Hemmer et al. 1999). The pathogenesis of the pulmonary oedema is classified as non-cardiogenic meaning that there is no indication of pulmonary hypertension or increased hydrostatic pressure associated with congestive heart failure (Wilkins et al. 2007). This implies a breakdown in the blood-air barrier probably as result of disruption of the endothelial cell layer, pneumocyte layer, or both. Endothelial activation- and inflammation-induced injury would be the most logical triggering mechanism, especially considering the significant accumulation of monocyte-macrophages throughout the lungs of infected dogs.

In this study, endothelial activation was present in all cases, being moderate in 54.5% of cases, mild in 27.3% of cases and severe in 18.2% of cases. Since direct injury by *B. rossi* parasites is unlikely as they have no mechanism to directly affect vascular endothelium, the injury was likely mediated by pro-inflammatory cytokines released from activated macrophages (e.g. IL-8, IL2, TNF- α and MCP-1). These cytokines have been shown in circulation in *B. rossi* infections previously in what typifies a 'cytokine storm' (Goddard et al. 2016; Leisewitz et al. 2019a). It seems likely therefore that an increase in these pro-inflammatory mediators may also be involved in destabilisation of the pulmonary endothelial layer in canine *Babesia*-associated ALI/ARDS by destabilising this cell layer's functional and anatomical integrity.

The VCAM-1 antigen is expressed on activated endothelial cells and it facilitates leukocyte migration and is upregulated by TNF- α (Woo et al. 2005) and HMGB-1 (Fiuza et al. 2003). It is important in the cyto-adherence of malaria-infected red blood cells to endothelial cells in the lungs and central nervous system of humans (Ockenhouse et al. 1992; Wu et al. 2011) and in mice (El-Assaad et al. 2013). In this study however, there was no clear difference in staining pattern between the controls and infected cases, but, of interest, was the visible granular staining noted on the cytoplasmic membranes of intravascular mononuclear leukocytes in the infected dog lungs. Research has shown that VCAM-1 can be expressed on cells other than endothelium (such as tissue macrophages, dendritic cells and even Kupffer cells in the liver in human patients) which may explain this finding (Kong et al. 2018). This might also explain the increase in serum VCAM-1 levels noted by Kuleš et al. (2017), but this requires further investigation.

Monocyte-macrophages were the predominant cell population noted, particularly in the alveolar walls and lumens. A severe mononuclear leukostasis was noted in the cases as well and there were often rafts of adhered mononuclear cells present in the larger bronchial vasculature. Most cases showed a moderate to severe increase in this phenotype in the interstitium and within the alveolar capillaries, which was associated with increased alveolar wall thickness. Further classification of this cell population was performed with CD204 and MAC387 immunohistochemistry.

CD204 is expressed in resident and tissue macrophages as well as dendritic cells (Kato et al. 2013). This marker showed an increase in alveolar macrophages of 7.4 \times over the normal controls as well as 5.3 \times and 0.4 \times increase in the alveolar walls and peribronchial regions, respectively. Since CD204 is a marker of tissue-resident macrophages, there is clear stimulation of these cells to proliferate in situ and there was a noticeable increase in mitotic frequency in some cases. The source of the stimulation is probably proinflammatory cytokine-related and is further discussed below.

MAC387 labels myeloid/histiocyte antigens expressed by circulating and tissue neutrophils, monocytes and reactive tissue macrophages and eosinophils but not dendritic cells (Brandtzaeg et al. 1988). MAC387 immunohistochemistry for bone marrow-derived monocyte-macrophages and polymorphonuclear leukocytes showed a major 10.8 \times increase compared to

the controls in the alveolar lumens and a 4 \times increase in the alveolar walls compared to the controls. Since neutrophils were minimally observed in histological sections, most of these cells were probably bone marrow-derived circulating monocytes. There was clearly significant extravasation of these cells into the alveolar lumens, likely in response to alveolar wall injury and subsequent haemorrhage, fibrin exudation and oedema. Their presence within the alveolar walls also may indicate a role in the immune reaction. They are an important source of cytokines for activation of the acute inflammatory response as a component of the innate immune system and they also trigger the adaptive immune response.

In most cases of ARDS, activation of alveolar macrophages with subsequent release of pro-inflammatory cytokines (such as IL-1, IL-8 and TNF-) is considered an essential step in the pathogenesis (Ware 2006, Ware & Matthay 2000). It is unclear how intravascular haemoprotozoan parasites such as *Babesia rossi* or *Plasmodium falciparum* cause activation of these alveolar macrophages but given that there are activated monocytes within the intravascular compartment, proinflammatory cytokine release from these cells is highly likely and it seems very probable that a cell phenotype important in parasite clearance is also involved in host damage (Chua et al. 2013). A transcriptomic study in an experimental *B. rossi* infection also demonstrated type I interferon upregulation (Smith et al. 2021). There may be spill-over into the alveolar compartment along with likely endothelial cell activation and injury leading to oedema, fibrin exudation and subsequent activation of alveolar macrophages. Another possibility is that the macrophages are not activated by the pro-inflammatory cytokines directly, but are triggered by the haemorrhage, fibrin and pulmonary oedema (which was consistently observed in these cases), in a futile attempt to clean up the spillage and restore function. This seems less likely given that a pro-inflammatory cytokine milieu is noted in cases of babesiosis (Goddard et al. 2016; Leisewitz et al. 2019a). The type of macrophage response may also be of interest. CD40+ (M1) macrophages were increased in patients with severe *Plasmodium falciparum* infections with pulmonary oedema compared to non-pulmonary oedema patients and there was no difference in CD163 (M2) macrophages between pulmonary oedema and non-pulmonary oedema patients (Klinkhamrhom et al. 2020).

In a murine model of malaria-associated ARDS, C57BL/6j mice infected with *Plasmodium berghei* showed interstitial oedema and leukocyte infiltration present on Day 8 post-infection (PI). By Day 10 PI, eosinophilic hyaline membranes were present (Van den Steen et al. 2010). The types of leukocytes encountered in the murine model were not established but are likely to be mononuclear cells similar to those seen in canine *Babesia*-associated ARDS. The oedema was also consistent between the two species. It is interesting that the dominant inflammatory cell response in classical human ALI/ARDS is the neutrophil (where bacteria and trauma are the most common triggers (Matthay & Zimmerman 2005)). This draws a clear distinction between the pathogenesis of ARDS associated with macrophagic inflammation in haemoprotozoan infections, versus the neutrophilic inflammation associated with more common bacterial and traumatic triggers.

Together, the CD3 and CD20 immunohistochemistry showed significantly more lymphocytes than initially observed with H&E staining. This suggests that lymphocytes may play a role in the interstitial inflammatory response in canine babesiosis. CD3 immunohistochemistry for T-lymphocytes showed a large 12.4 × increase in CD3-positive T-lymphocytes in the alveolar walls. This suggests that T-lymphocytes may be playing a significant role in the inflammation. T-lymphocytes are an essential component in cell-mediated immunity and may be activated in two ways. The first possible mechanism occurring via the classical pathway with T-helper 1 (T_h1) cells releasing IL-2 or IFN- γ , or, alternatively, but less likely, via T-helper 2 (T_h2) macrophages. Cytotoxic T-lymphocytes (CTLs) are also activated via the T_h1 pathway by the presentation of antigens on major histocompatibility complex-class I (MHC-1) with a co-stimulatory signal from an antigenic presenting cell. Activated CTLs can release perforins and granzymes inducing apoptosis in targeted cells and thus may be a cause of the single cell death (noted in some cases in the current study) but may also directly damage the vascular endothelium. The noticeable increase in T-lymphocytes is interesting, as in a recent study evaluating the peripheral lymphocyte phenotype in dogs naturally infected with *Babesia rossi*, dogs with complicated babesiosis showed a drop in CD3+ lymphocytes compared to cases with uncomplicated babesiosis (Rautenbach et al. 2017). The authors speculated that there may be functional immune suppression due to apoptosis or redistribution of the effector T-lymphocytes, or a combination of these and other mechanisms (Rautenbach et al. 2017). Although there was some single cell death in these cases, the clear increase in T-lymphocytes in the pulmonary tissue suggests that redistribution of lymphocytes may be a significant cause of the drop in peripheral T-lymphocyte cells noted in the previous study. In the spleen of dogs with lethal babesiosis, there was no significant difference in the T-lymphocyte populations in infected vs control cases. It would stand to reason that the spleen, being the primary organ responsible for clearing haemoprotozoan parasites, would become hyperplastic and the lack of an appreciable increase in T-cells may be due to rapid redistribution or accelerated apoptosis.

Haemorrhage was mild in 45.5% of cases, severe in 18.2% of cases, moderate in 18.2% of cases and severe in 18.2% of cases. The distribution of haemorrhage was multifocal in 77.8%, coalescing in 11.1% and diffuse in 11.1%. Most cases showed some form of haemorrhage which corresponded to the macroscopic pathology. Haemorrhage is not a common finding in dogs with ALI or ARDS (Balakrishnan et al. 2017). In these *Babesia*-infected dogs, it was likely the result of endothelial injury resulting from a macrophage-mediated cytokine storm (Colby et al. 2001). Severe thrombocytopenia and a bleeding tendency may have also contributed (Goddard et al. 2013).

Fibrin exudation into the alveolar lumen was absent in 45.5%, moderate in 27.3%, mild in 18.2% and severe in 9.1% of cases. This is not a common pathology in the lungs of dogs. It is described in association with respiratory epithelial damage caused by canid herpesvirus respiratory infections (Kumar et al. 2015) and in canine respiratory coronavirus (Priestnall 2020) as well as in dogs with naturally acquired African Horse Sickness

pneumonia (O'Dell et al. 2018). Fibrin exudation was seen in approximately half the cases, although why it was seen less frequently than haemorrhage is unclear. It is possible that some of the dogs were also in disseminated intravascular coagulation (Goddard et al. 2013) (another potential complication of *Babesia rossi* infection) and that severe coagulation factor depletion (through consumption) left insufficient thrombin to cleave fibrinogen. Alternatively, there was activation of the fibrinolytic system causing fibrinolysis and dissolution.

Although not a prominent finding, two of the cases (18.2%) did show evidence of intravascular thrombosis. Hypercoagulability is another potential complication of canine babesiosis (Goddard et al. 2013), but it is uncertain whether the thrombosis occurs secondary to pulmonary injury, induced hypercoagulability or a combination of both. A scintigraphic perfusion study of the lungs of uncomplicated cases of *B. rossi* infection also did not demonstrate obvious pulmonary thromboembolic disease (Sweers et al. 2008). Pulmonary thromboembolism is a feature of immune mediated haemolytic anaemia (IMHA) in dogs (Carr et al. 2002; Johnson et al. 1999) and babesiosis has been identified as a trigger of IMHA (Garden et al. 2019). Malaria has also been associated with both micro and macrovascular thrombosis (Schwameis et al. 2015).

Intra-erythrocytic *Babesia* parasites were visible in two cases but others showed no evidence of parasitaemia, this was likely due to anti-babesial treatment as the parasitaemia clears within 24 hours of diminazine aceturate treatment (Jacobson et al. 1996). Occasional intravascular megakaryocytes were also noted but this is not uncommon with systemic infections due to bone-marrow hyperplasia and shifting of immature blasts into systemic circulation.

There were a few important shortcomings in this study. Only lethal cases were included in this case series, so it is possible that sublethal pulmonary injury may be present in some cases of treated complicated and uncomplicated canine babesiosis that survive. Ante-mortem lung function data such as arterial blood gas and pulse oximetry were not available for these cases. All the cases were treated prior to death which has a major and rapid effect on parasite density (Jacobson et al. 1996), precluding judgement on the possibility of a direct interaction between parasitised erythrocytes and pulmonary vascular endothelial cells. Finally, electron microscopy of the endothelial barrier was not performed, but this would be the most logical avenue for future research.

Conclusion

Our findings were quite homogenous across the case series with most cases showing severe high protein content pulmonary oedema as well as moderate to severe, multifocal to coalescing alveolar haemorrhages and fibrin exudation. The haemorrhage and oedema extended into the alveolar ducts and bronchioles. Alveolar walls were diffusely thickened due to a marked increase in monocyte-macrophage inflammatory cells. There was a particularly marked increase in MAC387-positive bone marrow-derived monocytes and macrophages, and CD204-positive macrophages, as well CD3-positive T-lymphocytes

compared to the healthy controls. This indicates a role for both tissue and bone-marrow-derived monocyte-macrophages as well as T-lymphocytes in *Babesia*-related ALI/ARDS. Neutrophils did not play a significant role in the inflammation. This study also confirmed that the lung injury caused during natural complicated *Babesia rossi* infection in dogs fulfils the criteria for the definitions of ALI and ARDS (Wilkins et al. 2007). The lung pathology in the current study was similar to murine malaria-associated ARDS in C57BL/6J mice infected with *Plasmodium berghei* NK65 (Van den Steen et al. 2010), the murine model of *Babesia*-associated ALI/ARDS in C3H/HeN mice infected with WA-1 *Babesia* (Hemmer et al. 1999) as well as human malaria-associated ALI/ARDS (Spitz 1946; Taylor et al. 2012) and human babesiosis (Vannier et al. 2015). Hyaline membranes were not a feature in this study, probably due to the acute nature of the respiratory pathology and decreased survival of the dogs. The histology of this cohort of babesia-infected dogs did thus not fit all the criteria laid out for DAD in a recent review of this phenomenon in animals. The dogs described here met one of the three criteria for DAD (namely interstitial and intra-alveolar oedema as evidenced by a prominent lymphohistiocytic infiltrate in alveolar walls in particular as well as increased macrophages in alveolar lumens). Remarkable in absence was any evidence of hyaline membranes. Just over 50% of the babesia cases did however have variably dense infiltrates of fibrin in alveolar lumens which is a feature of exudative (acute) DAD (Carvalho & Stevenson 2022). These criteria are however only met in around 50% of human cases with ARDS (Carvalho & Stevenson 2022). This cohort does meet the veterinary criteria for the diagnosis of ARDS (Wilkins & Seahorn 2004; Wilkins et al. 2007). As in human malaria-associated ARDS, thrombosis and infarction were also rarely observed in canine babesiosis.

Conflict of interest

The authors have no competing interests to declare.

Funding source

This work was supported by funding provided by the South African National Research Foundation on grant CPR13080726333 held by A Leisewitz. The funding agency played no role in the research project or preparation of the manuscript for publication.

Ethical approval

This study was approved by the animal ethics committee of the University of Pretoria (V073-16).

ORCID

S Clift  <https://orcid.org/0000-0003-3965-5840>

A Leisewitz  <https://orcid.org/0000-0001-8432-9425>

References

Aitken, E.H., Negri, E.M., Barboza, R., et al., 2014, Ultrastructure of the lung in a murine model of malaria-associated acute lung injury/acute respiratory distress syndrome, *Malar J* 13, 230. <https://doi.org/10.1186/1475-2875-13-230>.

Anstey, N.M., Handoyo, T., Pain, M.C., et al., 2007, Lung injury in vivax malaria: pathophysiological evidence for pulmonary vascular sequestration and posttreatment alveolar-capillary inflammation, *J Infect Dis* 195(4), 589–596. <https://doi.org/10.1086/510756>.

Ashbaugh, D.G., Bigelow, D.B., Petty, T.L., et al., 1967, Acute respiratory distress in adults, *Lancet* 2, 319–323. [https://doi.org/10.1016/S0140-6736\(67\)90168-7](https://doi.org/10.1016/S0140-6736(67)90168-7).

Balakrishnan, A., Drobotz, K.J., Silverstein, D.C., 2017, Retrospective evaluation of the prevalence, risk factors, management, outcome, and necropsy findings of acute lung injury and acute respiratory distress syndrome in dogs and cats: 29

cases (2011–2013), *J Vet Emerg Crit Care* 27(6), 662–673. <https://doi.org/10.1111/vec.12648>.

Bancroft, J.D., Gamble, M., 2008, Theory and practice of histological techniques, Elsevier Health Sciences.

Brandtzaeg, P., Jones, D.B., Flavell, D.J., et al., 1988, Mac 387 antibody and detection of formalin resistant myelomonocytic L1 antigen, *J Clin Pathol* 41, 963–970. <https://doi.org/10.1136/jcp.41.9.963>.

Carr, A.P., Panciera, D.L., Kidd, L., 2002, Prognostic factors for mortality and thromboembolism in canine immune-mediated hemolytic anemia: a retrospective study of 72 dogs, *J Vet Intern Med* 16(5), 504–509. <https://doi.org/10.1111/j.1939-1676.2002.tb02378.x>.

Carvalho, F.R., Stevenson, V.B., 2022, Interstitial pneumonia and diffuse alveolar damage in domestic animals, *Vet Pathol* 59(4), 586–601. <https://doi.org/10.1177/03009858221082228>.

Castro, C.Y., 2006, ARDS and diffuse alveolar damage: A pathologist's perspective, *Semin Thorac Cardiovasc Surg* 18(1), 13–19. <https://doi.org/10.1053/j.semtcvs.2006.02.001>.

Chua, C.L.L., Brown, G., Hamilston, J.A., et al., 2013, Monocytes and macrophages in malaria: protection or pathology?, *Trends in Parasitol* 29(1), 26–34. <https://doi.org/10.1016/j.pt.2012.10.002>.

Colby, T.V., Fukuoka, J., Ewaskow, S.P., et al., 2001, Pathologic approach to pulmonary hemorrhage, *Ann Diagn Pathol* 5(5), 309–319. <https://doi.org/10.1053/adpa.2001.27923>.

El-Assaad, F., Wheway, J., Mitchell, A.J., et al., 2013, Cytoadherence of *Plasmodium berghei*-infected red blood cells to murine brain and lung microvascular endothelial cells in vitro, *Infect Immun* 81(11), 3984–3991. <https://doi.org/10.1128/IAI.00428-13>.

Fiuza, C., Bustin, M., Talwar, S., et al., 2003, Inflammation-promoting activity of HMGB1 on human microvascular endothelial cells, *Blood* 101(7), 2652–2660. <https://doi.org/10.1182/blood-2002-05-1300>.

Garden, O.A., Kidd, L., Mexas, A.M., et al., 2019, ACVIM consensus statement on the diagnosis of immune-mediated hemolytic anemia in dogs and cats, *J Vet Intern Med* 33(2), 313–334. <https://doi.org/10.1111/jvim.15441>.

Goddard, A., Leisewitz, A.L., Kjelgaard-Hansel, M., et al., 2016, Excessive pro-inflammatory serum cytokine concentrations in virulent canine babesiosis, *PLoS One* 11, 1–15. <https://doi.org/10.1371/journal.pone.0150113>.

Goddard, A., Wiinberg, B., Schoeman, J.P., et al., 2013, Mortality in virulent canine babesiosis is associated with a consumptive coagulopathy, *Vet J* 196(2), 213–217. <https://doi.org/10.1016/j.tvjl.2012.09.009>.

Hemmer, R.M., Ferrick, D.A., Conrad, P.A., 2000, Up-regulation of tumor necrosis factor-alpha and interferon-gamma expression in the spleen and lungs of mice infected with the human *Babesia* isolate WA1, *Parasitol Res* 86, 121–128. <https://doi.org/10.1007/s004360050021>.

Hemmer, R.M., Wozniak, E.J., Lowenstine, L.J., et al., 1999, Endothelial cell changes are associated with pulmonary edema and respiratory distress in mice infected with the WA1 human *Babesia* parasite, *J Parasitol* 85(3), 479–489. <https://doi.org/10.2307/3285783>.

Henning, A., Clift, S.J., Leisewitz, A.L., 2020, The pathology of the spleen in lethal canine babesiosis caused by *Babesia rossi*, *Parasite Immunol* 42(5), e12706. <https://doi.org/10.1111/pim.12706>.

Jacobson, L.S., Clarke, I.A., 1994, The pathophysiology of canine babesiosis: new approaches to an old puzzle, *J S Afr Vet Assoc* 65, 134–145.

Jacobson, L.S., Reyers, F., Berry, W.L., et al., 1996, Changes in haematocrit after treatment of uncomplicated canine babesiosis: a comparison between diminazene and trypan blue, and an evaluation of the influence of parasitaemia, *J S Afr Vet Assoc* 67, 77–82.

Johnson, L.R., Lappin, M.R., Baker, D.C., 1999, Pulmonary thromboembolism in 29 dogs: 1985–1995, *J Vet Intern Med* 13(4), 338–345. <https://doi.org/10.1111/j.1939-1676.1999.tb02192.x>.

Jubala, C., Wojcieszyn, J., Valli, V., et al., 2005, CD20 expression in normal canine B cells and in canine non-Hodgkin lymphoma, *Vet Pathol* 42, 468–476. <https://doi.org/10.1354/vp.42-4-468>.

Kato, Y., Murakami, M., Hoshino, Y., et al., 2013, The class A macrophage scavenger receptor CD204 is a useful immunohistochemical marker of canine histiocytic sarcoma, *J Comp Pathol* 148(2–3), 188–196. <https://doi.org/10.1016/j.jcpa.2012.06.009>.

Klinkhamrhom, A., Glaharn, S., Srisook, C., et al., 2020, M1 macrophage features in severe *Plasmodium falciparum* malaria patients with pulmonary oedema, *Malar J* 19, 182. <https://doi.org/10.1186/s12936-020-03254-0>.

Kong, D.H., Kim, Y.K., Kim, M.R., et al., 2018, Emerging roles of vascular cell adhesion molecule-1 (VCAM-1) in immunological disorders and cancer, *Int J Mol Sci* 19(4), 1057. <https://doi.org/10.3390/ijms19041057>.

Krause, P.J., Daily, J., Telford, S.R., et al., 2007, Shared features in the pathobiology of babesiosis and malaria, *Trends Parasitol* 23(12), 605–610. <https://doi.org/10.1016/j.pt.2007.09.005>.

Kuleš, J., Gotič, J., Mrljak, V., et al., 2017, Blood markers of fibrinolysis and endothelial activation in canine babesiosis, *BMC Vet Res* 13, 82. <https://doi.org/10.1186/s12917-017-0995-6>.

Kumar, S., Driskell, E., Cooley, A., et al., 2015, Fatal canid herpesvirus 1 respiratory infections in 4 clinically healthy adult dogs, *Vet Pathology* 52(4), 681–687. <https://doi.org/10.1177/0300985814556190>.

- Leisewitz, A., Goddard, A., De Gier, J., et al. 2019a. Disease severity and blood cytokine concentrations in dogs with natural *Babesia rossi* infection, *Parasite Immunol* 41(7), e12630. <https://doi.org/10.1111/pim.12630>.
- Leisewitz, A., Goddard, A., Clift, S., et al. 2019b. A clinical and pathological description of 320 cases of naturally acquired *Babesia rossi* infection in dogs, *Vet Parasitol* 271, 22–30. <https://doi.org/10.1016/j.vetpar.2019.06.005>.
- Leisewitz, A.L., Jacobson, L.S., De Moraes, H.S.A., et al., 2001, The mixed acid-base disturbances of severe canine babesiosis, *J Vet Intern Med* 15(5), 445–452. <https://doi.org/10.1111/j.1939-1676.2001.tb01573.x>.
- Lovegrove, F.E., Gharib, S.A., Pena-Castillo, L., et al., 2008, Parasite burden and CD36-mediated sequestration are determinants of acute lung injury in an experimental malaria model, *PLoS Pathog* 4, e1000068. <https://doi.org/10.1371/journal.ppat.1000068>.
- Maegraith, B., Gilles, H.M., Devakul, K., 1957, Pathological processes in *Babesia canis* infections, *Z Tropenmed Parasitol* 8, 485–514.
- Matjila, P.T., Leisewitz, A.L., Jongejan, F., et al., 2008, Molecular detection of tick-borne protozoal and ehrlichial infections in domestic dogs in South Africa, *Vet Parasitol* 155(1–2), 152–157. <https://doi.org/10.1016/j.vetpar.2008.04.012>.
- Matthay, M.A., Zimmerman, G.A., 2005, Acute lung injury and the acute respiratory distress syndrome, *Am J Respir Cell Mol Biol* 33(4), 319–327. <https://doi.org/10.1165/rcmb.F305>.
- O'Dell, N., Arnot, L., Janisch, C.E., et al., 2018, Clinical presentation and pathology of suspected vector transmitted African horse sickness in South African domestic dogs from 2006 to 2017, *Vet Rec* 182(25), 715–715. <https://doi.org/10.1136/vr.104611>.
- Ockenhouse, C.F., Tegoshi, T., Maeno, Y., et al., 1992, Human vascular endothelial cell adhesion receptors for *Plasmodium falciparum*-infected erythrocytes: roles for endothelial leukocyte adhesion molecule 1 and vascular cell adhesion molecule 1, *J Exp Med* 176(4), 1183–1189. <https://doi.org/10.1084/jem.176.4.1183>.
- Priestnall, S.L., 2020, Canine respiratory coronavirus: A naturally occurring model of COVID-19? *Vet Pathol* 57(4), 467–471. <https://doi.org/10.1177/0300985820926485>.
- Ramos-Vara, J., Miller, M., 2014, When tissue antigens and antibodies get along: revisiting the technical aspects of immunohistochemistry—the red, brown, and blue technique, *Vet Pathol* 51(1), 42–87. <https://doi.org/10.1177/0300985813505879>.
- Ramos-Vara, J., Miller, M., Valli, V., 2007, Immunohistochemical detection of multiple myeloma 1/interferon regulatory factor 4 (MUM1/IRF-4) in canine plasmacytoma: comparison with CD79a and CD20, *Vet Pathol* 44(6), 875–884. <https://doi.org/10.1354/vp.44-6-875>.
- Ramos-Vara, J.A., Kiupel, M., Baszler, T., et al., 2008, Suggested guidelines for immunohistochemical techniques in veterinary diagnostic laboratories, *J Vet Diagn Invest* 20, 393–413. <https://doi.org/10.1177/104063870802000401>.
- Rautenbach, Y., Goddard, A., Thompson, P.N., et al., 2017, A flow cytometric assessment of the lymphocyte immunophenotypes in dogs naturally infected with *Babesia rossi*, *Vet Parasitol* 241, 26–34. <https://doi.org/10.1016/j.vetpar.2017.05.001>.
- Schwameis, M., Schörgenhofer, C., Assinger, A., et al., 2015, Von Willebrand factor excess and ADAMTS13 deficiency: a unifying pathomechanism linking inflammation to thrombosis in DIC, malaria, and TTP, *Thromb Haemost* 113(4), 708–718. <https://doi.org/10.1160/TH14-09-0731>.
- Smith, R.L., Goddard, A., Boddapati, A., et al., 2021, Experimental *Babesia rossi* infection induces hemolytic, metabolic, and viral response pathways in the canine host, *BMC Genomics* 22, 619. <https://doi.org/10.21203/rs.3.rs-267384/v1>.
- Souza, M.C., Silva, J.D., Padua, T.A., et al., 2013, Early and late acute lung injury and their association with distal organ damage in murine malaria, *Respir Physiol Neurobiol* 186(1), 65–72. <https://doi.org/10.1016/j.resp.2012.12.008>.
- Spitz, S., 1946, The pathology of acute falciparum malaria, *Mil Surg* 99, 555–572. <https://doi.org/10.1093/milmed/99.5.555>.
- Sweers, L., Kirberger, R.M., Leisewitz, A.L., et al., 2008, The scintigraphic evaluation of the pulmonary perfusion pattern of dogs hospitalised with babesiosis, *JS Afr Vet Assoc* 79(2), 76–83. <https://doi.org/10.4102/jsava.v79i2.248>.
- Taylor, W.R., Hanson, J., Turner, G.D., et al., 2012, Respiratory manifestations of malaria, *Chest* 142(2), 492–505. <https://doi.org/10.1378/chest.11-2655>.
- Thille, A.W., Esteban, A., Fernandez-Segoviano, P., et al., 2013, Chronology of histological lesions in acute respiratory distress syndrome with diffuse alveolar damage: a prospective cohort study of clinical autopsies, *Lancet Respir Med* 1(5), 395–401. [https://doi.org/10.1016/S2213-2600\(13\)70053-5](https://doi.org/10.1016/S2213-2600(13)70053-5).
- Tomashefski Jr, J.F., 2000, Pulmonary pathology of acute respiratory distress syndrome, *Clin Chest Med* 21, 435–466. [https://doi.org/10.1016/S0272-5231\(05\)70158-1](https://doi.org/10.1016/S0272-5231(05)70158-1).
- Van den Steen, P.E., Deroost, K., Deckers, J., et al., 2013, Pathogenesis of malaria-associated acute respiratory distress syndrome, *Trends Parasitol* 29(7), 346–358. <https://doi.org/10.1016/j.pt.2013.04.006>.
- Van den Steen, P.E., Geurts, N., Deroost, K., et al., 2010, Immunopathology and dexamethasone therapy in a new model for malaria-associated acute respiratory distress syndrome, *Am J Respir Crit Care Med* 181(9), 957–968. <https://doi.org/10.1164/rccm.200905-0786OC>.
- Vannier, E.G., Diuk-Wasser, M.A., Ben Mamoun, C., et al., 2015, Babesiosis, *Infect Dis Clin North Am* 29(2), 357–370. <https://doi.org/10.1016/j.idc.2015.02.008>.
- Ware, L.B., 2006, Pathophysiology of acute lung injury and the acute respiratory distress syndrome, *Semin Respir Crit Care Med*, 27(4), 337–349. <https://doi.org/10.1055/s-2006-948288>.
- Ware, L.B., Matthay, M.A., 2000, The acute respiratory distress syndrome, *N Engl J Med* 342, 1334–1349. <https://doi.org/10.1056/NEJM200005043421806>.
- Welz, C., Leisewitz, A.L., Jacobson, L.S., et al., 2001, Systemic inflammatory response syndrome and multiple-organ damage/dysfunction in complicated canine babesiosis, *J S Afr Vet Assoc* 72(3), 158–162. <https://doi.org/10.4102/jsava.v72i3.640>.
- White, D.J., Talarico, J., Chang, H.G., et al., 1998, Human babesiosis in New York State: Review of 139 hospitalized cases and analysis of prognostic factors, *Arch Intern Med* 158, 2149–2154. <https://doi.org/10.1001/archinte.158.19.2149>.
- Wilkins, P.A., Otto, C.M., Baumgardner, J.E., et al., 2007, Acute lung injury and acute respiratory distress syndromes in veterinary medicine: consensus definitions: The Dorothy Russell Havemeyer Working Group on ALI and ARDS in Veterinary Medicine, *J Vet Emerg Crit Care* 17(4), 333–339. <https://doi.org/10.1111/j.1476-4431.2007.00238.x>.
- Wilkins, P.A., Seahorn, T., 2004, Acute respiratory distress syndrome, *Vet Clin North Am Equine Pract* 20(1), 253–273. <https://doi.org/10.1016/j.cveq.2003.11.001>.
- Woo, C.H., Lim, J.H., Kim, J.H., 2005, VCAM-1 upregulation via PKC δ -p38 kinase-linked cascade mediates the TNF- α -induced leukocyte adhesion and emigration in the lung airway epithelium, *Am J Physiol Lung Cell Mol Physiol* 288, L307–L316. <https://doi.org/10.1152/ajplung.00105.2004>.
- Wu, Y., Szestak, T., Stins, M., 2011, Amplification of *P. falciparum* cytoadherence through induction of a pro-adhesive state in host endothelium, *PLoS One* 6, e24784. <https://doi.org/10.1371/journal.pone.0024784>.